Mechanical properties and microstructure of Ti–6.5Al–2Zr –1Mo–1V/TiB composites produced by vacuum arc or selective laser melting

M. S. Ozerov · V. S. Sokolovsky · D. G. Shaysultanov · I. A. Astakhov · S. V. Zherebtsov

Received: 6 August 2024 / Accepted: 3 September 2024 / Published online: 19 November 2024

Abstract
Ti–6.5Al–2Zr–1Mo–1V/TiB metal-matrix composites were produced by vacuum arc or selective laser melting (SLM) methods using 0.7 and 2 wt.% TiB_2 in the charge mixture. The initial microstructure of the as-cast and SLM composites consisted of TiB fibers randomly distributed within the two-phase α/β matrix. The average apparent length and cross-sectional size of the TiB fibers in the as-cast composite with 0.7 wt.% TiB_2 and as-cast composite with 2 wt.% TiB_2 were ~10 and ~11 μm and ~ 1.0 and ~ 1.2 μm, respectively. The average apparent length and cross-sectional size of the TiB fibers in the SLM composite with 0.7 wt.% TiB_2 and the SLM composite with 2 wt.% TiB_2 were ~3.5 and ~4.0 μm and ~0.2 and ~0.25 μm, respectively. The addition of the TiB fibers resulted in 20–27% increase in the strength without visible decrease in the ductility. An unreinforced alloy produced by the SLM showed 60% increase in strength compared to that obtained by the vacuum arc melting. The addition of the TiB fibers resulted in ~30% increase in the strength (for both composites) with a decrease in the ductility to 8 and 3% for the SLM composite with 0.7 wt.% TiB_2 and the SLM composite with 2 wt.% TiB_2, respectively.

Keywords Titanium alloy · Vacuum arc melting · Selective laser melting · Metal-matrix composite · Boride fibers · Microstructure · Mechanical properties

Introduction

Titanium and titanium-based alloys are widely used in shipbuilding and aerospace industries due to their high specific strength, high corrosion resistance, and good manufacturability [1, 2]. And more importantly, high-temperature titanium alloys can be used for the production of parts, such as aircraft turbine compressors, which operate at elevated temperatures. However, a noticeable decrease in the strength characteristics at temperatures of 500–600°C, which is mainly due to the lack of high-temperature hardening mechanisms, limits the application of these alloys. Specifically, the operating temperatures of a well-known high-temperature near-alpha Ti–6.5Al–2Zr–1Mo–1V alloy are below 500 °C [3]. Increasing the heat resistance of the titanium alloys is simultaneously fundamental and technical problem, the solution of which opens up the possibility for these alloys to replace partially much heavier steels and nickel alloys [1–4].

A promising approach to an increase in the high-temperature strength of titanium alloys is the creation of metal-matrix composites (MMCs) by introducing refractory and strong ceramic phases into the ductile titanium matrix [5, 6]. One of the most promising reinforcements is provided by TiB particles which (i) are well matched with the titanium matrix without the formation of a transition region, (ii) have a close thermal expansion

coefficient, and (iii) provide increased strength even at elevated temperatures due to good thermal stability of TiB [5–7]. Specifically, the TiB reinforced MMCs can be used at temperatures by 100–200 °C higher than those of usual industrial high-temperature titanium alloys, reaching the operating temperature range of 600–800 °C [8].

An important factor influencing the morphology of borides and structure of the matrix and directly affecting the mechanical properties of the composites is the MMCs production method. For example, the sizes of borides formed during the casting process can be quite large both due to a relatively slow cooling rate and hypereutectic composition of the Ti–TiB system. The formation of large needle-like precipitates can decrease the ductility and crack resistance of the MMCs [7, 9]. In contrast, the short processing time and high cooling rate during selective laser melting (SLM) resulted in the formation of much smaller borides [10, 11]. In addition, some obvious difference in the structure can be caused by the different approach itself, i.e. powder metallurgy (SLM) and usual casting (vacuum arc melting) [12]. Earlier investigations [10–13] also showed rather high strength properties of the Ti–TiB MMCs obtained by the SLM. However, there is practically no information on the effect of the amount of borides on the microstructure and mechanical properties of composites obtained by the SLM. Therefore, the aim of the present work is the examination of the effect of production method (casting vs. SLM) on the structure and mechanical properties of the TiB reinforced Ti–6.5Al–2Zr–1Mo–1V alloy at room temperature.

Material and methods

Laboratory scale ingots (50 g) of the Ti–6.5Al–2Zr–1Mo–1V composite were produced using the vacuum arc melting of pure (≥ 99.9 wt.%) Ti, Al, Zr, Mo, and V granules with 0.7 and 2 wt.% commercial purity (CP) powder of TiB_2 (99.9 wt.%). CP powders of Ti–6.5Al–2Zr–1Mo–1V alloy (99.9 wt.% with size ~100 µm) and TiB_2 (99.99 wt.% with size ~6 µm) were used for the selective laser melting of the Ti–6.5Al–2Zr–1Mo–1V composites (Fig. 1). A powder mixture contained Ti–6.5Al–2Zr–1Mo–1V (base) with 0.7 and 2 wt.% TiB_2 produced using a Retsch RS200 vibrating cup mill in ethanol at a milling rotation speed of 700 rpm and a milling time of 1 h. The SLM of the composites was carried out in an argon atmosphere using a 3D printer DMP Flex 200 with a 316L steel plate used as a substrate. The flow rate of argon (used as shielding gas) was 5 l/min. To improve the quality of the workpieces, the direction of the laser beam movement changed by 67° during fusion of each subsequent layer. The distance between tracks and the beam diameter were 50 and 70 µm, respectively. For the sake of comparison, unreinforced (i.e. without addition of TiB_2) Ti–6.5Al–2Zr–1Mo–1V alloy specimens were also fabricated using both vacuum arc melting and SLM. The notation of the investigated materials is presented in Table 1.

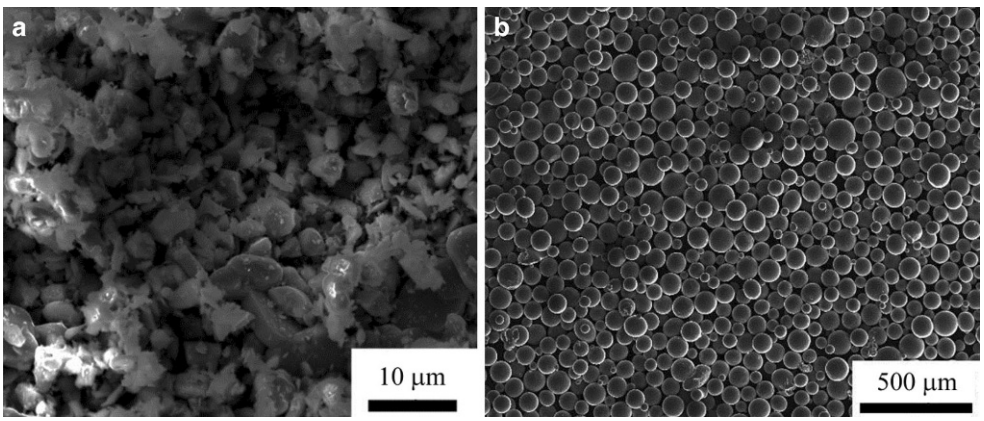

Fig. 1 SEM images of TiB_2 (**a**) and Ti–6.5Al–2Zr–1Mo–1V powders (**b**)

Table 1 Notation of the Investigated Materials

Condition	Marking
Ti–6.5Al–2Zr–1Mo–1V alloy produced by the vacuum arc melting	AC alloy
Ti–6.5Al–2Zr–1Mo–1V composite with 0.7 wt.% TiB_2 produced by vacuum arc melting	AC-0.7 composite
Ti–6.5Al–2Zr–1Mo–1V composite with 2 wt.% TiB_2 produced by vacuum arc melting	AC-2 composite
Ti–6.5Al–2Zr–1Mo–1V alloy produced by the selective laser melting	SLM alloy
Ti–6.5Al–2Zr–1Mo–1V composite with 0.7 wt.% TiB_2 produced by the elective laser melting	SLM-0.7 composite
Ti–6.5Al–2Zr–1Mo–1V composite with 2 wt.% TiB_2 produced by the selective laser melting	SLM-2 composite

The samples measured $4 \times 4 \times 6\,mm^3$ were cut from the produced materials. Then the specimens were compressed at room temperature at a nominal strain rate of 10^{-3} s^{-1} to destruction. Microstructures of the composites were examined using a FEI Quanta 600 scanning electron microscope (SEM) in backscattered electron (BSE) and secondary electron (SE) regimes. Specimens for the SEM were prepared by careful mechanical polishing; to reveal borides in the structure of the composites (in the SE regime), deep etching (for ~6 min) was carried out with Kroll's reagent (95% H_2O, 3% HNO_3, 2% HF). The Digimizer software was used to determine the average length or diameter of borides. In each condition, at least 400 measurements were carried out.

Results and discussion

The initial microstructure of the AC composites consisted of TiB fibers randomly distributed within the two-phase α/β matrix (Fig. 2a–d). The volume fraction of the β phase did not exceed 4% in all AC composites. The average apparent length and cross-sectional size of the TiB fibers in the AC-0.7 and AC-2 composites were ~10 and ~11 μm and ~1.0 and ~1.2 μm, respectively (Fig. 2a–d). The values of the volume fraction of the TiB fibers increased slightly from 6 to 8% for the AC-2 composite compared to the AC-0.7 composite. A two-phase α/β structure of the matrix was also obtained in the SLM composites, but the sizes of the borides were found to be significantly smaller (Fig. 2e–h). For example, the average apparent length and cross-sectional size of the TiB fibers in the SLM-0.7 and SLM-2 composites were ~3.5 and ~4.0 μm and ~0.2 and ~0.25 μm, respectively. The volume fraction of borides also decreased to 4 and 5% for the SLM-0.7 and SLM-2 composites, respectively. Sporadic particles of unreacted TiB_2 (Fig. 1e,h) were found in the structure of the both SLM composites, thereby suggesting not quite complete $Ti + TiB_2 = 2TiB$ in-situ reaction [5–7, 12].

Alloying with borides significantly affected the mechanical properties in compression at room temperature (irrespective of the production method) of the composites as compared to the unreinforced alloys (Fig. 3 and Table 2). For example, the non-reinforced AC alloy demonstrated the yield strength, peak strength, and compression ductility of 800 MPa, 1350 MPa, and 15%, respectively. The addition of TiB fibers resulted in 20 and 27% increase in strength without a visible drop in ductility for the AC-0.7 and AC-2 composites, respectively (Fig. 3a and Table 2). A similar trend was observed for the composites obtained by the SLM. However, there was an even greater increase in the strength properties with a slight drop in the plasticity values (Fig. 3b and Table 2). The non-reinforced SLM alloy demonstrated the yield strength, peak strength, and compression ductility of 1310 MPa, 1830 MPa, and 13%, respectively. Alloying with the TiB fibers resulted in ~30% (for both composites) increase in the strength with the decrease of ductility to 8 and 3% for the SLM-0.7 and SLM-2 composites, respectively (Fig. 3b and Table 2). It should be noted that the strength characteristics obtained in this work were found to be significantly higher in comparison with the composites obtained by the SLM in earlier works [10, 11, 13].

The results obtained clearly show a positive effect of borides on the strength of the Ti–6.5Al–2Zr–1Mo–1V alloys produced by different methods, in accord with some earlier results [14, 15]. For example, for the composites obtained by the vacuum arc melting, a moderate increase in the strength was observed with no

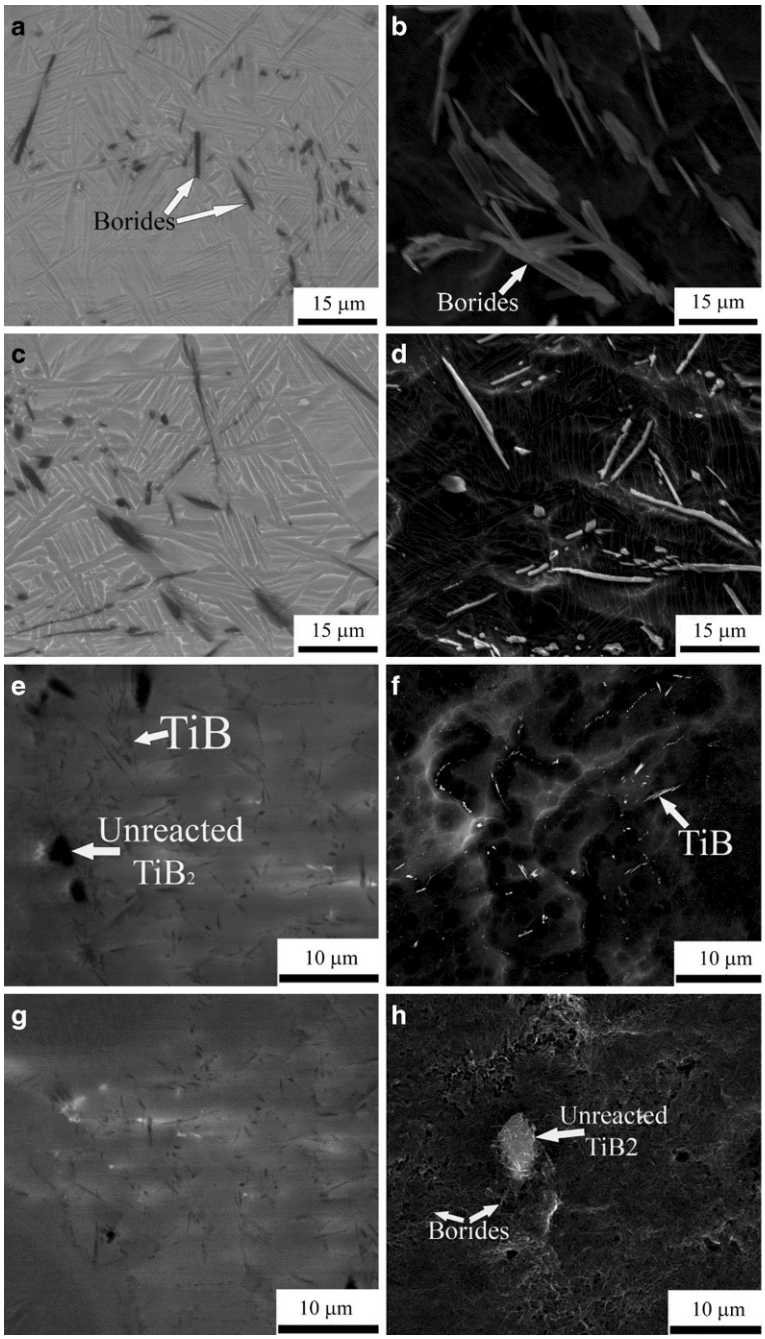

Fig. 2 SEM images of the microstructure of AC-0.7 (**a**,**b**), AC-2 (**c**,**d**), SLM-0.7 (**e**,**f**), and SLM-2 composites (**g**,**h**) for the polished (**a**,**c**,**e**,**g**) and etched surfaces (**b**,**d**,**f**,**h**)

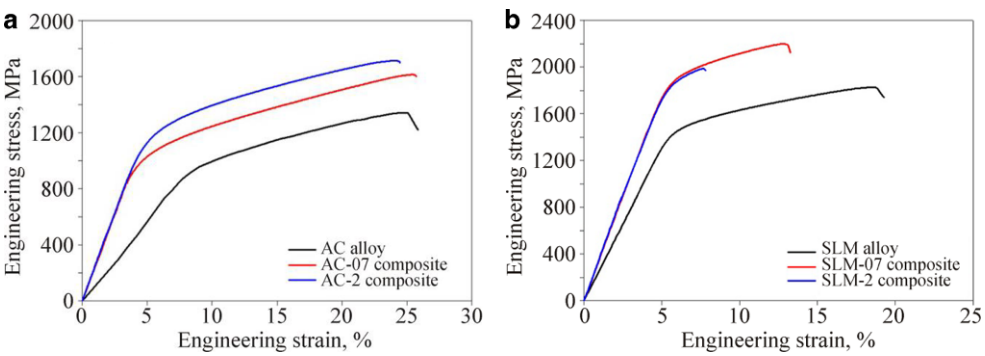

Fig. 3 Engineering stress-strain curves obtained during compression of the as-cast alloys (**a**) and SLM alloys (**b**) at 20 °C

Table 2 Mechanical Properties in Compression of the AC Alloy, AC-0.7 Composite, AC-2 Composite, SLM Alloy, SLM-0.7 Composite, and SLM-2 Composite at room temperature

Condition	Yield strength, MPa	Peak strength, MPa	ε, %
AC alloy	800 ± 20	1350 ± 35	18 ± 3
AC-0.7 composite	920 ± 22	1620 ± 42	17 ± 3
AC-2 composite	1020 ± 25	1720 ± 45	16 ± 3
SLM alloy	1310 ± 32	1830 ± 49	13 ± 2
SLM-0.7 composite	1720 ± 45	2200 ± 52	8 ± 1.5
SLM-2 composite	1700 ± 44	1990 ± 50	3 ± 0.5

decrease in the ductility compared to the AC alloy, which is very important. It is worth noting that the SLM alloy showed 60% higher strength compared to the AC alloy. More importantly, the ductility did not decrease dramatically. Thus, the SLM is a very promising process for producing parts of TiB reinforced titanium alloys. Slightly different results were obtained for the composites produced by the SLM. The tendency toward an increase in the strength compared to the unreinforced SLM alloy was noted, similar to the composites obtained by the vacuum arc melting. However, a drop in the ductility by 40 and 80% was observed for the SLM-0.7 and SLM-2 composites, respectively. It is quite possible that this drop in the plastic characteristics occurred due to the incomplete in-situ reaction of the boride synthesis, as evidenced by the presence of unreacted TiB_2 particles in the structure of the SLM composites. In any case, a very high increase in the strength of the SLM composites at room temperature allows us to consider the SLM to be a very promising approach to producing MMCs.

Conclusions

The initial microstructure of the as-cast composites consisted of the TiB fibers randomly distributed within the two-phase α/β matrix. The average apparent length and cross-sectional size of the TiB fibers in the as-cast composite with 0.7 wt.% TiB_2 and as-cast composite with 2 wt.% TiB_2 were ~10 and ~11 μm and ~1.0 and ~1.2 μm, respectively. The values of the volume fraction of the TiB fibers increased slightly from 6 to 8% for the as-cast composite with 2 wt.% TiB_2 compared to the as-cast composite with 0.7 wt.% TiB_2. A two-phase α/β structure was also obtained in the SLM composites, but the sizes of the borides were found to be significantly smaller. The average apparent length and cross-sectional size of the TiB fibers in the SLM composite with 0.7 wt.% TiB_2 and SLM composite with 2 wt.% TiB_2 were ~3.5 and ~4.0 μm and ~0.2 and ~0.25 μm, respectively. The volume fraction of borides also decreased to 4 and 5% for the SLM composite with 0.7 wt.% TiB_2 and SLM composite with 2 wt.% TiB_2, respectively. Particles of unreacted TiB_2 were found in the structure of both SLM composites.

Alloying with borides significantly affected the mechanical properties in compression of the composites at room temperature compared to the unreinforced alloys. The addition of the TiB fibers resulted in 20 and 27% increase in the strength without a visible drop in the ductility for the as-cast composite with 0.7 wt.% TiB_2 and as-cast composite with 2 wt.% TiB_2, respectively. The non-reinforced SLM alloy demonstrated the yield strength, peak strength, and compression ductility of 1310 MPa, 1830 MPa, and 13%, respectively. Alloying with the TiB fibers resulted in ~30% increase in strength (for both composites) with a decrease in the ductility to 8 and 3% for the SLM composite with 0.7 wt.% TiB_2 and the SLM composite with 2 wt.% TiB_2, respectively.

Institutional review board statement Applicable.

Acknowledgements The authors gratefully acknowledge the financial support from the Russian Science Foundation (Grant Number 23-49-00108). The authors are grateful to the personnel of the Joint Research Centre, Belgorod State University for their assistance with the instrumental analysis.

Funding This work was supported by the Russian Science Foundation (Grant No. 23-49-00108; https://rscf.ru/project/23-49-00108).

Author Contribution M.S.O. and S.V.Z. conceived of the presented idea, developed the theory, and performed the computations; V.S.S., D.G.Sh. and I.A.A. carried out the experiments; M.S.O. wrote the manuscript with support from S.V.Z.; M.S.O., V.S.S., and S.V.Z., conceived the study and were in charge of overall direction and planning. All authors discussed the results, contributed to the final manuscript, and have read and agreed to the published version of the manuscript.

Conflicts of interest The authors declare that they have no known competing financial interests or personal relationships that could have appeared to influence the work reported in this paper.

References

1. Williams, J.C., Boyer, R.R.: Opportunities and issues in the application of titanium alloys for aerospace components. Metals (Basel). **10**, 705 (2020). https://doi.org/10.3390/met10060705
2. Pushp, P., Dasharath, S.M., Arati, C.: Classification and applications of titanium and its alloys. Mater. Today: Proc. **54**, 537–542 (2022). https://doi.org/10.1016/j.matpr.2022.01.008
3. Sun, Q.J., Xie, X.: Microstructure and mechanical properties of TA15 alloy after thermo-mechanical processing. Mater. Sci. Eng. A **724**, 493–501 (2004). https://doi.org/10.1016/j.msea.2018.03.109
4. Sun, Z., Yang, H.: Microstructure and mechanical properties of TA15 titanium alloy under multi-step local loading forming. Mater. Sci. Eng. A **523**, 184–192 (2009). https://doi.org/10.1016/j.msea.2009.05.058
5. Chandran, R.K.S., Panda, K.B., Sahay, S.S.: TiB_w-reinforced Ti composites: Processing, properties, application, prospects, and research needs. JOM **56**, 42–48 (2004). https://doi.org/10.1007/s11837-004-0127-1
6. Godfrey, T., Goodwin, P., Ward-Close, C.: Titanium particulate metal matrix composites—reinforcement, production methods, and mechanical properties. Adv. Eng. Mater. **2**, 85–91 (2000). https://doi.org/10.1002/(SICI)1527-2648(200003)2:3⟨85::AID-ADEM85⟩3.0.CO;2-U
7. Morsi, K.: Review: Titanium–titanium boride composites. J Mater Sci **54**, 6753–6771 (2019). https://doi.org/10.1007/s10853-018-03283-w
8. Zhang, C.J., Kong, F.T., Xu, L.J.: Temperature dependence of tensile properties and fracture behavior of as-rolled TiB/Ti composite sheet. Mater. Sci. Eng. A **556**, 962–969 (2012). https://doi.org/10.1016/j.msea.2012.07.110
9. Ozerov, M., Stepanov, N., Sokolovsky, V.: Deformation behavior and microstructure evolution of a TiB-Reinforced Ti–6.5Al–2Zr–1Mo–1V Matrix. Compos. Met. (basel). **13**, 1812 (2023). https://doi.org/10.3390/met13111812
10. Attar, H., Löber, L., Funk, A.: Mechanical behavior of porous commercially pure Ti and Ti–TiB composite materials manufactured by selective laser melting. Mater. Sci. Eng. A **625**, 350–356 (2015). https://doi.org/10.1016/j.msea.2014.12.036
11. Attar, H., Bönisch, M., Calin, M.: Selective laser melting of in situ titanium–titanium boride composites: Processing, microstructure and mechanical properties. Acta Mater **76**, 13–22 (2014). https://doi.org/10.1016/j.actamat.2014.05.022
12. Huang, L., An, Q., Geng, L.: Multiscale architecture and superior high-temperature performance of discontinuously reinforced titanium matrix composites. Adv. Mater. **33**(6), 2000688 (2020). https://doi.org/10.1002/adma.202000688
13. Attar, H., Prashanth, K.G., Zhang, L.C.: Effect of powder particle shape on the properties of in-situ Ti–TiB composite materials produced by selective laser melting. J. Mater. Sci. Technol. **31**(10), 1001–1005 (2015). https://doi.org/10.1016/j.jmst.2015.08.007
14. Tsang, H.T.: Effects of volume fraction of reinforcement on tensile and creep properties of in-situ TiB/Ti MMC. Scr. Mater. **37**(9), 1359–1365 (1997). https://doi.org/10.1016/S1359-6462(97)00251-0
15. Wang, S., Huang, L.J., Geng, L.: Significantly enhanced creep resistance of low volume fraction in-situ TiBw/Ti6Al4V composites by architecture network reinforcements. Sci Rep **7**, 40823 (2017). https://doi.org/10.1038/srep40823

Authors and Affiliations

M. S. Ozerov[1] · V. S. Sokolovsky[1] · D. G. Shaysultanov[1] · I. A. Astakhov[1] · S. V. Zherebtsov[1]

✉ M. S. Ozerov
ozerov@bsu.edu.ru

V. S. Sokolovsky
sokolovskiy@bsu.edu.ru

D. G. Shaysultanov
shaysultanov@bsu.edu.ru

I. A. Astakhov
astakhov@bsu.edu.ru

S. V. Zherebtsov
zherebtsov@bsu.edu.ru

[1] Belgorod National Research University, Belgorod, Russian Federation